Chapter 5

The production of prototypical MOFs from waste-PET provides a stepping-stone towards MOFs-based water-harvesting applications

Jianwei Ren [a, *], Tien-Chien Jen [a], Wojciech Starosta [b], Bożena Sartowska [b], Philiswa Nosizo Nomngongo [c]

[a]*University of Johannesburg, Johannesburg, Kingsway, and University Road, Auckland Park, 2092, P.O. Box 524, Auckland Park, 2006, Johannesburg, South Africa*

[b]*Laboratory of Materials Research, Institute of Nuclear Chemistry and Technology, Dorodna 16, 03-195 Warsaw, Poland*

[c]*Department of Chemical Sciences, University of Johannesburg, Doornfontein Campus, P.O. Box 17011, Johannesburg, 2028, South Africa*

**Corresponding author. Tel: +27 11 559 2103. Email: jren@uj.ac.za (J. Ren)*

Abstract

Metal-organic frameworks (MOFs)-based atmospheric water harvesting (AWH) has become an interesting research topic to address water scarcity in the arid regions. However, the availability of the cost-effective prototypical MOFs materials poses an actual challenge for their wide applications. In this work, the production of prototypical MOFs from waste PET is recognised as an important stepping-stone towards MOFs-based AWH applications.

Keywords: Metal-organic frameworks, Atmospheric water harvesting, Prototypical MOFs, Waste PET

1. Global warming affects the water scarcity

A popular quote by Leonardo da Vinci acknowledges that water is a driving force of nature, and people use water for almost everything. It is a precious commodity. Water scarcity has been a global systemic risk that is developing over time. As a result, six billion people will face different levels of water scarcity during a certain number of months per year by

2050 [1,2]. Some intensive discussions and strong evidence have linked the specific events or an increase in their numbers to the human influence on climate changes, such as non-stopping CO_2 emission in a short time [3]. As shown in Figure 1, the research conducted by Kummu *et al.* [4] found that the population facing water scarcity has increased by nearly 16-fold since the 1900s although the population increased only 4-fold. In particular, the improved living standards and the pursuit for economic growth have been attributed to the water scarcity. Global warming essentially has a negative impact on the water cycles.

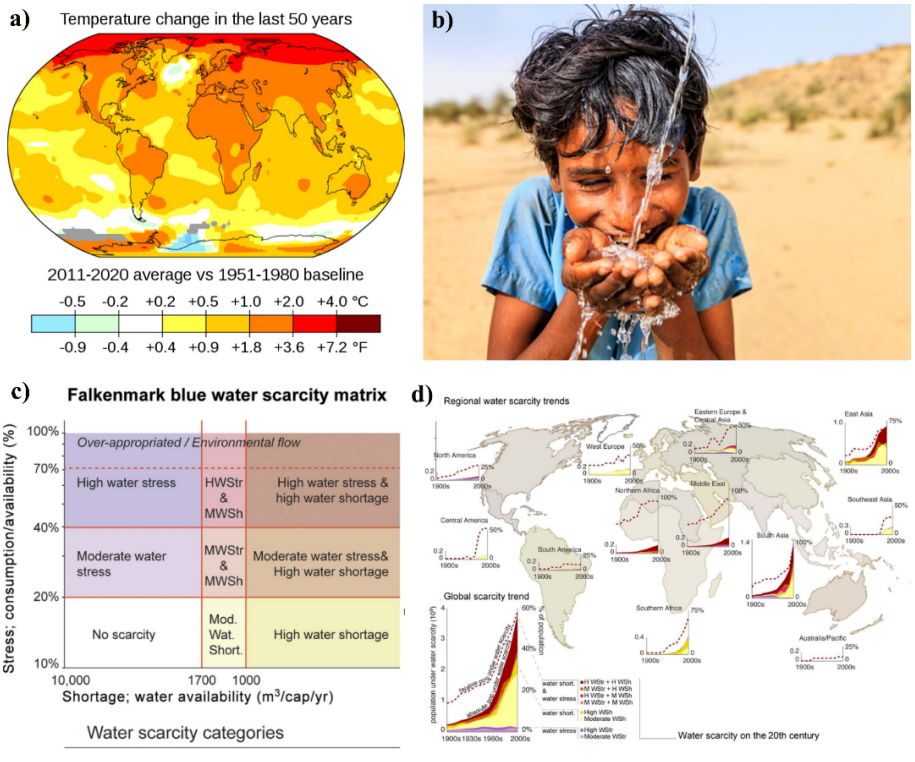

Figure 1: a) Temperature changes in the last 50 years. b) Global warming essentially is a water story. c) Adopted water scarcity matrix, d) Regional and global water scarcity trajectories. Reproduced with permission from ref 1. Copyright ©2016 Springer Nature Limited.

Clearly, water is an ultimately finite resource, so its scarcity has posed a more serious threat than is currently acknowledged. Scientific, technological, and philosophical advances will certainly alleviate future freshwater scarcity. Regardless of these factors, global warming and associated changes to the water cycle vastly complicate the challenge of

sustaining freshwater supplies for the foreseeable future. Although global warming has so far not been fully reflected, it is responsible for the visible sea-ice loss. Extreme events such as heatwaves, drying soil, and a change in climate are evidence of global warming, and the climate models have consistently projected temperature increases in tropical countries over the coming decades. More specifically, it was projected that poor countries that have contributed minimally to climate change will experience more increase in variability, and this would amplify the inequality associated with the impact of a changing climate. As a matter of climate justice, it is essential for the relatively wealthy to bear the expenses for digging deeper wells, paying for the electricity consumption, and treating lower-quality freshwater [5,6]. Similar to the oil war, the freshwater scarcity threat will eventually turn into comprehensive debates and political conflicts in many countries in the arid regions of the globe, and the more critical local patterns than global patterns will make the problem more difficult to solve. From the literature point of view, one local-focus rather than a global-focus remedial measure can be proposed to support a more sustainable population and economic growth: using the atmospheric water as a freshwater resource in arid regions globally.

2. The atmospheric water as freshwater resource in different forms

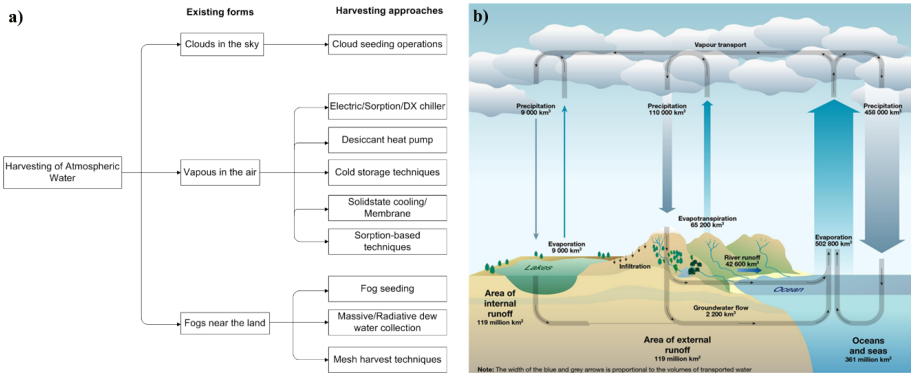

Figure 2: a) Atmospheric water exists in three main forms. b) The isotopic composition of atmospheric water vapour.

As shown in Figure 2, about 10^{21} litres of water exist in the atmosphere at any given time in three basic forms – clouds floating in the sky, fog close to the land, and water vapour in the air.

More liquid water likely tends to become atmospheric water under global warming conditions. Theoretically, this portion of water has the

potential to water the arid regions of the world. Unlike the desalination process, minimum influence may disrupt the hydrological cycle when water is taken out of the air [7]. Besides, the source of the atmospheric water is normally clean, and the water quality is high enough to make the water suitable for drinking and other domestic or agricultural purposes [8]. In other words, atmospheric water harvesting seems to be a geographically and climatically independent water production method for disaster relief needs and decentralised water supply. The demonstrations on atmospheric water harvesting have been made in several traditional ways, such as artificial rain or cloud seeding for cloud water harvesting, fog seeding or mesh techniques for fog water harvesting, and dew water harvesting using water bamboo tower. Traditionally, the harvesting of fog water and dew water was achieved with clear economic feasibility in areas with high humidity, fog gathering, or cloud cover [9].

In humid regions, water vapour can be condensed and harvested in the form of dew water by cooling it on a surface below its dew point temperature. Usually, the cooling technologies are classified as passive cooling, solar-regenerated desiccant, and active cooling. Ideally, when the water is taken out of the air, there is minimum influence to disrupt the hydrological cycle or steal water away from important critical sources nearby. In fact, the fog is a cloud but with physical contact with the surface of the earth, and the harvesting of water occurs when the fog droplets impact and intercept the harvesting surfaces. In other words, although fog water harvesting promises to be a low-cost approach for drinking water, crop irrigation, livestock watering , and forest restoration in dryland mountains, it is highly dependent on the geographical factors and conditions for fog occurrence. Typically, the combination of an ocean with a near-coast mountainous region is favourable for such fog harvesting. Clearly, the setting-up of such a system for fog water harvesting is subject to limited rain at least for a significant time period of a year [10].

By referring to the project demonstrations of fog harvesters in Figure 3a, the mesh types design (Figure 3b) play a critical role in determining the system efficiency, and the appropriate tuning of the wetting characteristics of the surfaces, reducing the wire radii and optimising the wire spacing, all lead to more efficient fog harvesting [12]. Figure 3c illustrates the project demonstrations for fog water harvesting in arid or seasonally arid regions. In this regard, Jarimi and co-workers [13] have done comprehensive work by reviewing the critical aspects of the fog harvesters, including design, efficiency and feasibility studies, mesh topology, surface wettability, as well as biomimicry-inspired fog water harvesters. With the prerequisite of temperature below its saturation point, only a limited number of places where fog can be naturally formed from moist air provided that. In fact, the fog was

reported as an alternative freshwater source less accessible than seawater. Besides, although dew water can be extracted from the air by cooling to a temperature lower than the air dew point, several stepping-stone works reported that the energy consumption is high, especially when solar energy is used due to low convention efficiency, low specific yields (SY), and low daytime relative humidity (RH). However, a target with average daily drinking water of five litres per day per person can be achieved experimentally in the demonstration of materials-based atmospheric water harvesting [14]. Apparently, a local-focus rather than global-focus remedial measure can be proposed to support more sustainable population and economic growths, that is, using materials-based techniques to collect the atmospheric water as a freshwater resource in arid regions globally.

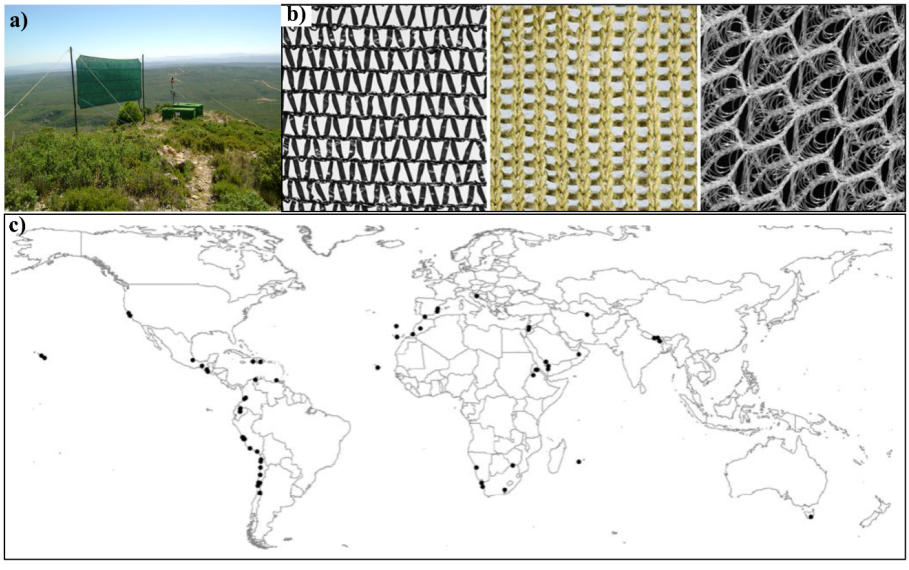

Figure 3: a) The project demonstration of the fog harvester. b) The used mesh for the fog water collection. c) Project demonstrations for fog water harvesting in arid or seasonally arid regions. Re-organised from ref [10, 11].

The relative humidity (Ø) represents the ratio of the partial pressure of water vapour (P_w) to the saturation pressure (P_s), while the absolution humidity (ω) represents the maximum amount of water that can be extracted from the air [15].

$$\emptyset = \frac{P_w}{P_s(T)} \tag{1}$$

The relation between relative humidity, absolute humidity, temperature, and total air pressure can be described using equation (2).

$$\emptyset = \frac{\omega P}{(0.622+\omega)P_s(T)} \quad (2)$$

3. Materials-based atmospheric water harvesting (AWH)

3.1. Working principle of materials-based AWH

The traditional AWH in humid regions can be realised by using fog harvest or by condensation. However, in regions with low RH below 30%, it is mandatory to bring down the air temperature below the freezing point, and such direct cooling of air to condense water turns out to be energy-consuming and impractical. It requires untenable amounts of electrical power to operate the refrigeration units. Apparently, this requires an effective way to concentrate the water vapour at acceptable energy consumption. As illustrated in Figure 4a, for the AWH in the arid regions with RH around 20% (*point a*), it must be cooled to the dew point (*point b*) to allow the water saturation. In contrast, for the AWH in the humidity regions with RH around 90% (*point c*), the cooling is minimal towards (*point d*). The employment of materials will essentially lift the desert air with low RH (*point a*) up to the high RH (*point c*) and then reaches the water saturation more efficiently than direct cooling. Generally, the direct cooling approach is applicable in the green region, and the materials-based can work in the pink region to turn the desert air into tropical air for further AWH purposes. Thus far, almost all the technology explorations have been focusing on the humid conditions in the green region with the principles of direct air cooling by using the condensation cycle. In other words, the direct cooling approach is only applicable in limited regions globally as shown in Figure 4b. In contrast, the materials-based AWH is capable of facilitating water harvesting from the air and delivering clean water. Accordingly, some materials, including inorganic salts, zeolites, porous silica, and composite matrices were tested to solve the dew point issue that has posed challenges for them to be implemented at lower RH conditions [16,17]. However, the literature revealed that all these materials pose different challenges in reality. These include slow-onset start, slow adsorption/desorption kinetics, low AWH capacity at low RH, and require extensive desorption energy.

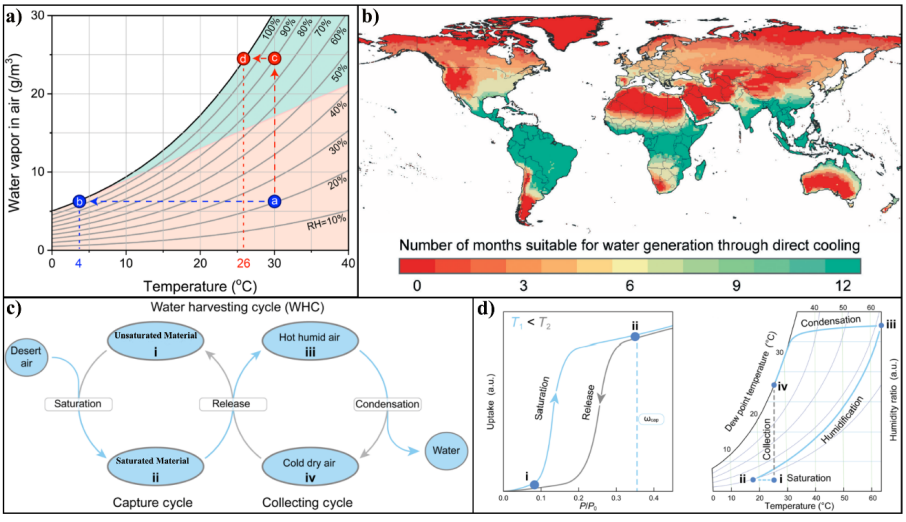

Figure 4: a) The modified psychrometric chart and b) The applicable regions for direct cooling. c) Materials-based AWH consists of the capture and collecting cycles. d) The capture cycle is defined by the sorption isotherm of the applied sorbent material, and the collecting cycle is defined by the psychrometric chart. Modified from Ref. [18-20] with permissions.

The materials-based AWH provides the possible capacity for water vapour concentration by materials beds from the air, which can later be recovered in a thermal-driven step. As shown in Figure 4c, a materials-based AWH cycle consists of a capture cycle and a collecting cycle. The unsaturated adsorbent materials will get saturation when exposed to air at night, and the water is released from the saturated sorbent materials when exposed to sunlight at daytime. The collection cycle takes place when the released water vapour humidifies the air in the vicinity of the materials at daytime, and liquefied water can be collected on the condenser under the function of condensation. This means , the materials-based AWH systems have the potential to be operated in arid regions by using a low-grade thermal energy source and achieving a low specific energy consumption per unit mass water production [21]. Being an efficient AWH system, firstly, it shall accommodate the general global scenario of being able to harvest atmospheric water at low humidity. Secondly, the adsorption-desorption kinetics of the water cycle shall be sufficient to allow the production of sufficient water. Thirdly, the working capacity should be high enough for the sake of energy saving for cycling. Currently, the most popular materials are represented by inorganic salts, zeolites, and porous polymers. Besides, many efforts had focused on the development strategies of superior

adsorbent materials and system designs with sustainable considerations. Clearly, in Figure 4d, the capture cycle is determined by the sorption isotherm of the sorbent materials, and the collection cycle is defined by the psychrometric chart. It is worth noting that the collection cycle can continue until the humidity ratio is too low to reach the dew point.

3.2. Criteria for materials-based AWH applications

The discussions above show that there are prerequisites for a high-performance AWH system such as a type IV or type V water adsorption isotherm with minimal or no hysteresis, a steep uptake below 25% with a high adsorption capacity below 35%, and ideally a significant shift of the inflection point for isotherms recorded at different temperature. The specialised materials play a key role in those processes. The key here is not just the amount of water absorbed, but also the amount that can be released via low-grade heat sources.

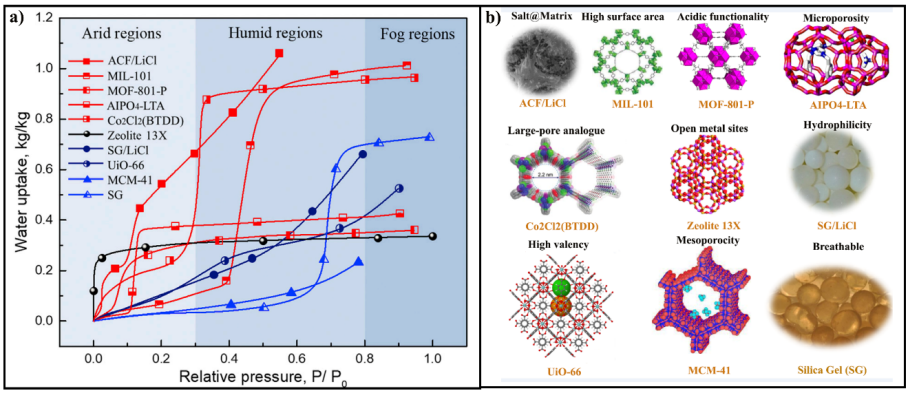

Figure 5: a) The promising materials reported in the literature for AWH. b) Different functionalities for materials design. Reproduced from Ref. [22] with permission.

As atmospheric water harvesting depends mainly on ambient relative humidity (RH), three applicable regions are usually discussed in the literature: fog regions with RH >80%, humid regions with 30%<RH<80%, and arid regions with RH<30%. As illustrated in Figure 5 [22], examples of materials like UiO-66 MOF with high valency perform well in the fog regions, MIL-101 MOF with high surface area performs well in the humid regions and the activated carbon fiber (ACF)/LiCl type of salt@matrix composite can perform well in both humid and arid regions. As summarised by De Lange *et al.* [23] and Burtch *et al.* [24], the criteria for the materials development to be used for water adsorption/desorption applications are: (i) S-shape of the water adsorption isotherm at 298 K. (ii) High

water sorption capacity at low humidity <30% RH. (iii) Low regeneration temperature <100 °C. (iv) High pore volume. This is desirable for improved performance, and the consistent microstructures will ensure a stepped absorption performance within a narrow RH range. (v) Adsorption steps should be located in the pressure range $0.1<p/p_0<0.3$, which not only increases the temperature lift but also decreases the desorption temperature. (vi) Hysteresis between adsorption and desorption branches should be avoided if possible. (vii) The materials should show a stable adsorption/desorption performance over thousands of cycles.

The sudden water uptakes in S-shape isotherm mean that the adsorbent can be regenerated by lower temperature heat sources. The narrow RH interval is well in accordance with the fixed working conditions of the adsorptive chiller. However, an open system usually experiences a very wide range of weather conditions during one day or through a whole year, and in such a case, an S-shape isotherm with a lower RH at the onset of the isotherm is necessary to equip the ability to collect sufficient water under any climate conditions. To maximise the capacity, a linear isotherm is expected for dehumidification, whose uptake will increase along with the rising RH.

Based on the above analysis, the ideal adsorbent material for water vapour harvesting applications should have features as follows: (i) in the adsorption process (<25 °C), their water sorption capacity should increase linearly with RH and (ii) in the desorption process (>35 °C), their water sorption capacity should drop steeply with increased temperature (S-type isotherms). From the literature point of view, the current commercial and laboratory available materials are difficult to fully satisfy these features, which are either temperature-insensitive or RH-sensitive. Some composite materials have been reported as a useful approach to designing high-performance, temperature-sensitive materials for water vapour harvesting [25-27]. Through open adsorbing metal sites and binding water prior to pore filling, the pore diameter can be effectively reduced to the critical diameter. In the review work conducted by Zhou *et al* [28], the materials-based AWH mechanism, fundamental requirements, and structural design principles were summarised into the general four aspects that include high water uptake, face capture/release, low energy demand, and cycling stability.

3.2. Selection of prototypical MOFs for AWH applications

For the selection of the optimal sorbent materials, several critical properties such as hydrophilicity, pore diameter, and stability must be taken into consideration [29]. In choosing a sorbet material, a balance

between the high affinity for water vapour and desorption energy must be struck. In this regard, metal-organic frameworks (MOFs) as a new generation of porous materials are able to accommodate all these required flexibilities and tune the water uptake step by varying factors such as pore size and hydrophilicity for water vapour harvesting applications in arid regions. Typically, the pore hydrophilicity of the selected MOFs shall be sufficient to allow the water nucleation and the pore-filling under the arid condition (<30% RH). Canivet *et al* [30] suggested disclosing the underlying mechanism by using three parameters including (i) the Henry constant (K_H) related to the slope of the adsorption isotherm at very low water partial pressures, (ii) the relative pressure at which half of the total water capacity is reached, and the maximum water adsorption capacity (). Typically, the Henry constant K_H mainly describes the surface adsorption properties, and pore-filling pressure mostly reflects the pore size. Clearly, both of them are correlated to reflect the hydrophobicity-hydrophilicity of the MOF material, which can be modified by the linker functionalisation. The total water uptake is correlated with the porous volume at the exception of MOFs with gate- opening properties and superhydrophobicity such as ZIF-8. For the water adsorption under a given temperature, the pore diameter shall be smaller than the critical diameter of 20 Å of the water molecule to avoid the undesirable hysteresis upon water desorption, which can be estimated from the equation:

$$D_c = 4\sigma T_c/(T_c - T) \tag{3}$$

where refers to the size of the water molecule, T is the temperature, and Tc = 647 K is the bulk critical temperature for water.

In other words, given a case of water vapour adsorption at room temperature, the critical apparent pore diameterdetermining the mechanism of adsorption is expected to be around 20 Å. Beyond this value, the pore-filling will occur through irreversible capillary condensation accompanied by capillary hysteresis loops, and below this critical diameter, pore-filling is continuous and reversible unless the MOF material exhibits some adsorption-induced flexibility. Fundamentally, this implies that an adsorbent with a pore diameter around 20 Å will result in the water pre-adsorption on the open metal sites prior to pore-filling. The sequential pore-filling starts from the smallest pore and progresses to the middle and largest pores. Thereafter, the internal available volume can be maximised for filling with water while avoiding irreversible capillary condensation. This serves as a general strategy in designing superior sorbents to proceed with a reversible pore filling [31]. An observed step water uptake

behaviour on MOF-801 and MOF-841 at 10% RH implied a spectacular binding of water at desert air condition. Further investigations showed the initial formation of pore shape-dependent water aggregates in the MOF pores, and these aggregates later served as the seeds to attract the additional water molecules into the pores [32]. Overall, the formation of those water seeds drove the isotherm into a step profile by contributing to the enhancement of water binding. Attributing by the polar secondary building units (SBUs) and nonpolar organic linkers, the release of water was enabled under mild conditions by following a cooperative mechanism as indicated by the step isotherm behaviour.

Unlike other materials and technologies, MOFs are the only materials known to work anytime and anywhere. The main challenge for MOF industrialisation is the negative view on large-scale MOF production in a cost-effective manner. There seems to be a general tendency and misconception that all MOFs are unstable to water, polar solvents, too expensive, and low yielding to scale up. Cost reduction will be possible if a mass production process can be developed.

4. Prototypical MOFs production from waster-PET provides an important stepping-stone

Costs are crucial to determine the business case and viability of any commercial application. MOFs are really compelling in terms of performance, but right now the scalability to larger volumes is limited for certain types and the cost is also high. In traditional forms of MOF synthesis such as solvothermal methods, a very wide space is required to tune the reaction parameters such as reaction temperature, time, stoichiometry, and so on. Generally, the availability of cost-effective MOFs remains a real challenge in the wide implementation of MOFs-based AWH systems (Figure 6).

So far, a library of MOFs has been reported to display a broad variety of behaviour for water adsorption applications, and these earlier works provided the main guidelines for the design of MOFs with specific hydrophilicity-hydrophobicity properties. Table 1 lists the water affinities of MOF samples from the hydrophilic HKUST-1 MOF to the very hydrophobic MOF ZIF-8. The mesoporous MIL-101 showed an exceptional water capacity of 1 g g^{-1} [33]. The large water capacity of MIL-101 exhibited an adsorption isotherm of combined type I and type V. Such isotherms consist of two steps starting from the water adsorption at the inorganic clusters (type I) and followed by the filling of the mesoporous cavities (type V) [34,35].

Figure 6: Pilot-scale production of cost-effective MOFs remains a knowledge gap

Some of the earlier work focused on the green synthesis of the target MOFs. Chen *et al.* [37] reported an aqueous solution-based synthesis of prototypical UiO-66-NH_2 at room temperature, which offered the advantages such as reduction of toxic byproducts, reduction of operation costs, and increased safety in the MOF production. Zhao and co-workers [38] used HNO_3 as an additive to produce prototypical MIL-101(Cr) in >100 g quantities with yields near 70% and BET-surface areas around 4000 $m^2\ g^{-1}$. Recently, research has been focused on the chemical engineering aspects of MOF production.

Table 1: MOFs studied in literature for AWH applications

MOFs	SA[a] ($m^2\ g^{-1}$)	V_p [b] ($cm^3\ g^{-1}$)	Uptake capacity [c] ($g\ kg^{-1}$)	Working capacity [d] ($g\ kg^{-1}$)	Water desorbed (%)
MIL-125(Ti)	1153	0.47	323	313	97
MIL-125(Ti)-NH_2	1358	0.55	413	409	99
UiO-66(Zr)	959	0.40	347	338	97
UiO-66(Zr)-NH_2	1109	0.46	364	355	98
MOF-808(Zr)	1880	0.69	744	714	96
MIL-101(Cr)	2579	1.63	1263	1246	98

MOFs	SA[a] ($m^2 g^{-1}$)	V_p[b] ($cm^3 g^{-1}$)	Uptake capacity[c] ($g kg^{-1}$)	Working capacity[d] ($g kg^{-1}$)	Water desorbed (%)
HKUST-1(Cu)	1512	0.41	218	105	48
MIL-53(Al)	814	0.41	13	2	15
ZIF-8(Zn)	1835	0.69	15	6	40

[a]Surface area calculated from Brunauer-Emmett-Teller (BET) model analysis of N_2 gas adsorption-desorption isotherm at 77 K. [b]Pre volume calculated at p/p_0=0.4 of N_2 adsorption isotherm (77 K). [c]Water vapor uptake capacity was determined gravimetrically, nad the value is taken from the first cycle adsorption at 70% RH and 22 °C at ambient pressure. [d]Working capacity was determined gravimetrically by the difference in the amount of water desorbed and adsorbed during water cycle stability and recovery studies. Modified from Ref. [36].

4.1. Proof-of-concept of prototypical MOFs production from waste PET

The terephthalic acid (BDC) after being retrieved from plastic bottles was tested by gas chromatography (GC) which showed that the concentration was more than 99%, which is comparable to that of commercial BDC. This recycled BDC was used as the organic ligand in the synthesis of MIL-53 (Fe). After the initial proof-of-concept was approved by producing MOFs from the clear PET [39–40], experimental trials were conducted on the coloured waste PET and food trays. The results are shown in Figure 7.

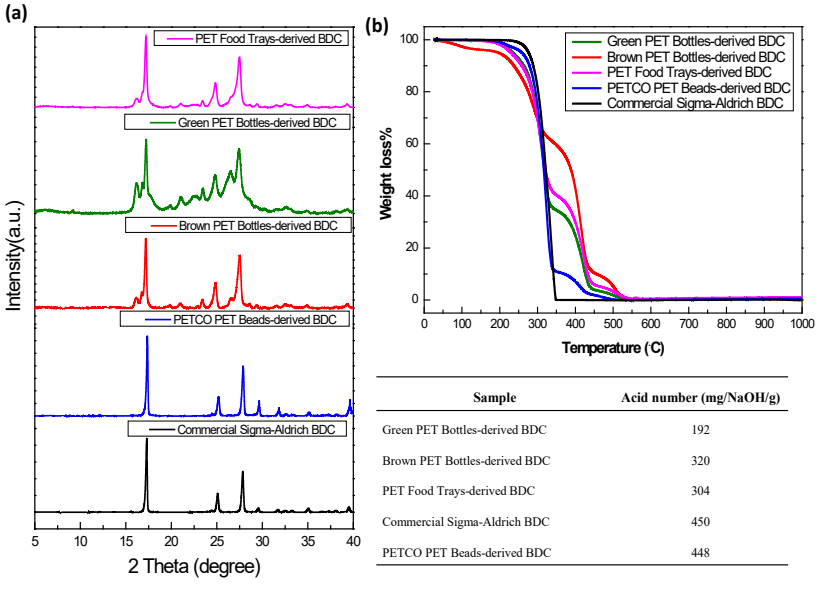

Sample	Acid number (mg/NaOH/g)
Green PET Bottles-derived BDC	192
Brown PET Bottles-derived BDC	320
PET Food Trays-derived BDC	304
Commercial Sigma-Aldrich BDC	450
PETCO PET Beads-derived BDC	448

Figure 7: (a) PXRD patterns, and (b) TGA curves of the BDC samples derived from different PET sources. Right bottom Table: the titration results of the acid numbers from different BDC samples

Figure 7 shows the X-ray diffraction (XRD) patterns and the thermogravimetric analysis (TGA) curves of the BDC products from different PET sources. As compared to the commercial Sigma-Aldrich BDC sample with a purity of 98%, the crystallinity of PETCO PET Beads-derived BDC is very close to that of the commercial BDC, as evidenced by the similar acid number of 448 mg NaOH/g against 450 mg NaOH/g. As indicated by the XRD patterns, the crystallinity of the Brown PET Bottles derived-BDC sample is close to that of the PET Food Trays-derived BDC sample. Meanwhile, the containing acid numbers are also nearly the same. In contrast, the crystallinity of the Green PET Bottles-derived BDC is the lowest with an acid number of only 192 mg NaOH/g. It can be seen from Figure 7b that the purity of different BDC samples are slightly different.

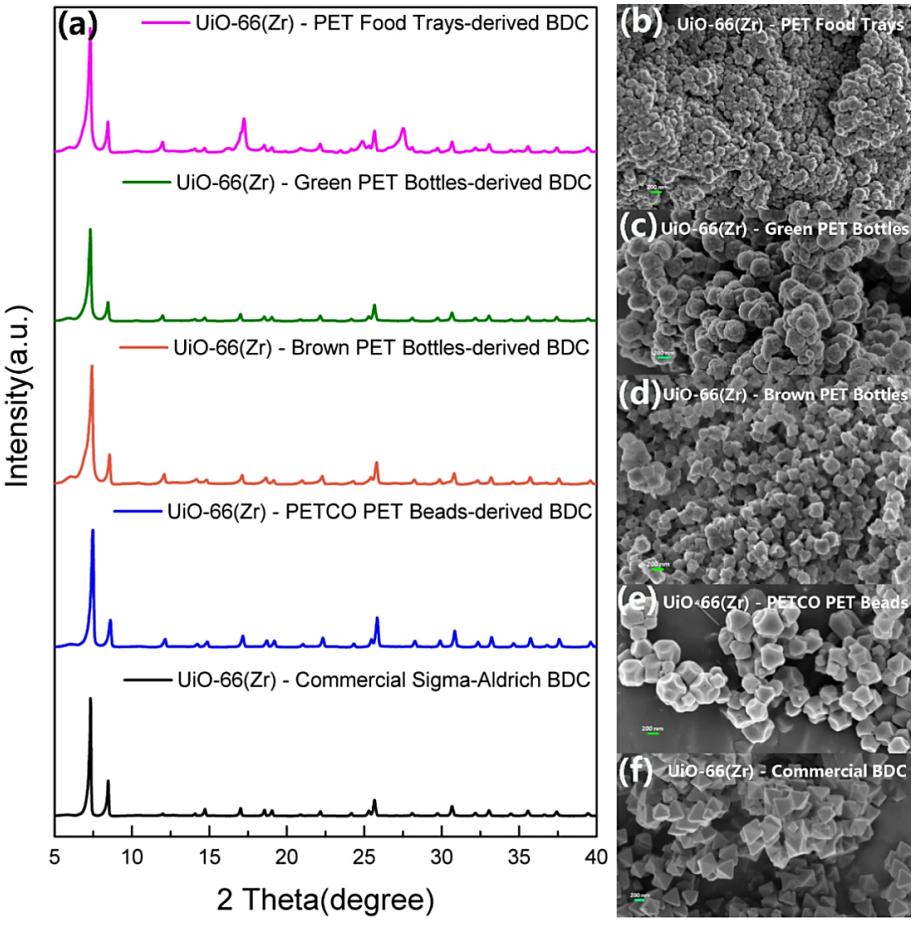

Figure 8: (a) XRD patterns, and (b-f) SEM images of the Zr-MOF samples prepared from different BDC sources

Several characteristic reflection signals in Figure 8a confirmed the successful synthesis of MOF UiO-66(Zr) from different PET-derived BDC when compared to the simulated XRD pattern. The relative crystallinities of the obtained MOF UiO-66(Zr) samples are comparable to that from commercial BDC feedstock from Sigma-Aldrich. However, as shown in Figure 8b, the Zr-MOF sample synthesised from Green PET Bottles-derived BDC shows the lowest relative crystallinity. The scanning electron microscope (SEM) images in Figure 8b-f show the quite differed morphologies of the obtained MOF UiO-66(Zr) samples.

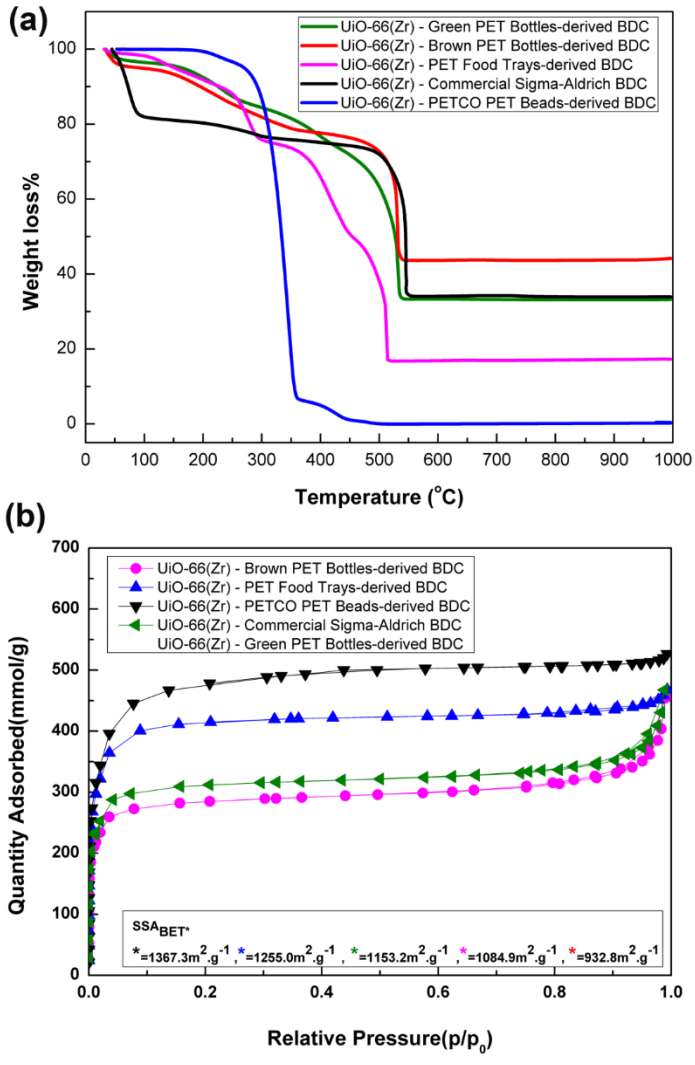

Figure 9: (a) TGA curves and (b) N_2 sorption of the MOF UiO-66(Zr) samples prepared from different BDC sources.

Figure 9a shows the TGA properties of the obtained MOF UiO-66(Zr) prepared from different BDC sources. The N_2 and H_2 sorption isotherms presented in Figure 9b indicate that all the PET-derived MOF UiO-66(Zr) materials have relatively lower N_2 and H_2 adsorption levels, but the obtained values are comparable to that from the commercial feedstock as well as other previously developed MOF UiO-66(Zr) materials. MOF UiO-66(Zr) samples were also synthesised from the coloured PET bottles-derived BDC, where the effects of additives and colorants should be considered on the textural properties of the prepared MOF UiO-66(Zr). The experiment

results suggested that the MOF UiO-66(Zr) samples from the clear PET food trays-derived BDC have lower textural properties than those from the clear PET beads-derived BDC. The reason could be the effects of additives and colorants from the green and brown coloured bottles.

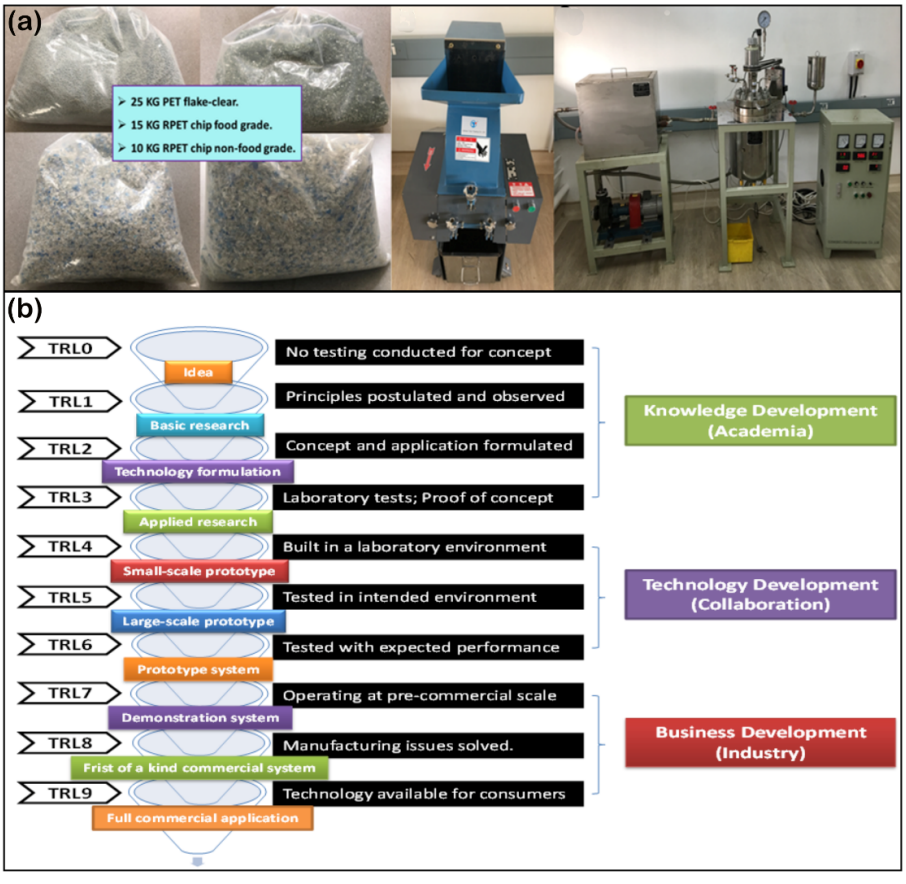

Figure 10: (a) Upscaled production of the target MOFs from waste-PET. (b) The technology readiness level (TRL).

With that knowledge in hand, the prototypical MOFs production was scaled-up to 1 kg/batch in our laboratory, as illustrated in Figure 10a, and the technology readiness level (TRL) referring to Figure 10b can be defined between 6–7.

5. Conclusion

In summary, this work experimentally demonstrated the production of prototypical MOFs materials from various waste PET streams including the PET food trays, green and brown PET bottles. The results provided

a stepping-stone towards the implementation of MOFs-based AWH systems.

References

1. Mekonnen, M.M.; Hoekstra, A.Y. Four billion people facing severe water scarcity. *Sci Adv* **2016**, 2, e1500323. https://doi.org/10.1126/sciadv.1500323
2. Boretti, A.; Rosa, L. Reassessing the projections of the world water development report. *npj Clean Water* **2019**, 2, 15. https://doi.org/10.1038/s41545-019-0039-9
3. D. Coumou, S. Rahmstorf. A decade of weather extremes. *Nat Clim Change* **2012**, 2, 491–496. https://doi.org/10.1038/nclimate1452
4. Kummu, M.; Guillaume, J.H.A.; de Moel, H.; Eisner, S.; Flörke, M.; Porkka, M.; Siebert, S.; Veldkamp, T.I.E.; Ward, P.J. The world's road to water scarcity: shortage and stress in the 20th century and pathways towards sustainability. *Sci Rep* **2016**, 6, 38495. https://doi.org/10.1038/srep38495
5. Bathiany, S.; Dakos, V.; Scheffer, M.; Lenton, T.M. Climate models predict increasing temperature variability in poor countries. *Sci Adv* **2018**, 4, eaar5809. https://doi.org/10.1126/sciadv.aar5809
6. Wada, Y.; de Graff, I.E.M.; van Beek, L.P.H. High-resolution modelling of human and climate impacts on global water resources. *J Adv Model Earth Syst* **2016**, 8, 735–763. https://doi.org/10.1002/2015MS000618
7. Nikolayev, V.S.; Beysens, D.; Gioda, A.; Milimouka, I.; Katiushin, E.; Morel, J.P. Water recovery from dew. *J Hydrol.* **1996**, 182, 19–35. https://doi.org/10.1016/0022-1694(95)02939-7
8. Khalil, B.; Adamowski, J.; Shabbir, A.; Jang, C.; Rojas, M.; Reilly, K.; Ozga-Zielinski, B. A review: dew water harvesting from radiative passive collectors to recent developments of active collectors. *Sustain Water Resour. Manag.* **2016**, 2, 71–86. https://doi.org/10.1007/s40899-015-0038-z
9. Habeebullah, B.A. Potential use of evaporator coils for water extraction in hot and humid areas. *Desalination* **2009**, 237, 330–345. https://doi.org/10.1016/j.desal.2008.01.025
10. Klemm, O.; Schemenauer, R.S.; Lummerich, A.; Cereceda, P.; Marzol, V.; Corell, D.; van Heerden, J.; Reinhard, D.; Gherezghiher, T.; Olivier, J.; Osses, P.; Sarsour, J.; Frost, E.; Estrela, M.J.; Valiente, J.A.; Fessehaye, G.M. Fog as a fresh-water resource: overview and perspectives. *AMBIO* **2012**, 41, 221–234. https://doi.org/10.1007/s13280-012-0247-8

11. Choiniere-Shields, E (2013). The cloud harvester catches and stores fresh water from fog. From http://inhabitat.com/httpinhabitat-comwpadminpost-phppost519497actioneditmessage1/
12. Park, K.-C.; Chhatre, S.S.; Srinivasan, S.; Cohen, R.E.; McKinley, G.H. Optimal design of permeable fiber network structures for fog harvesting. *Langmuir* **2013**, 29, 13269–13277. https://doi.org/10.1021/la402409f
13. Jarimi, H.; Powell, R.; Riffat, S. Review of sustainable methods for atmospheric water harvesting. *Int J Low-Carbon Technol* **2020**, 15, 253–276. https://doi.org/10.1093/ijlct/ctz072
14. Lord, J.; Thomas, A.; Treat, N.; Forkin, M.; Bain, R.; Dulac, P.; Behroozi, C.H.; Mamutov, T.; Fongherser, J.; Kobilansky, N.; Washburn, S.; Truesdell, C.; Lee, C.; Schmaelzle, P.H. Global potential for harvesting drinking water from air using solar energy. *Nature* **2021**, 598, 611–617. https://doi.org/10.1038/s41586-021-03900-w
15. Gengel, Y.A.; Boles, M.A. Thermodynamics: an engineering approach 6th edition (SI units). The McGraw-Hill Companies, Inc., New York, 2007.
16. Yu, N.; Wang, R.; Lu, Z., Wang, L. Development and characterization of silica gel-LiCl composite sorbents for thermal energy storage. *Chem Eng Sci* **2014**, 111, 73–84. https://doi.org/10.1016/j.ces.2014.02.012
17. Ng, E.-P.; Mintova, S. Nanoporous materials with enhanced hydrophilicity and high water sorption capacity. *Microporous Mesoporous Mater* **2008**, 114, 1–26. https://doi.org/10.1016/j.micromeso.2007.12.022
18. Liu, C.-H.; Nguyen, H.L.; Yaghi, O. Reticular chemistry and harvesting water from desert air. AsiaChem 2020, 1, 18–25. https://doi.org/10.51167/acm00007
19. Xu, W.T.; Yaghi, O.M. Metal-organic frameworks for water harvesting from air, anywhere, anytime. *ACS Cent Sci* **2020**, 6, 1348–1354. https://doi.org/10.1021/acscentsci.0c00678
20. Fathieh, F.; Kalmutzki, M.J.; Kapustin, E.A.; Waller, P.J.; Yang, J.; Yaghi, O.M. Practical water production from desert air. *Sci Adv* **2018**, 4, No. eaat3198. https://doi.org/10.1126/sciadv.aat3198
21. William, G.E.; Mohamed, M.H.; Fatouh, M. Desiccant system for water production from humid air using solar energy. *Energy* **2015**, 90, 1707–1720. https://doi.org/10.1016/j.energy.2015.06.125
22. Tu Y.D.; Wang, R.Z.; Zhang, Y.N.; Wang, J.Y. Progress and expectation of atmospheric water harvesting. *Joule* **2018**, 2, 1452–1475. https://doi.org/10.1016/j.joule.2018.07.015

23. de Lange, M.F.; Verouden, K.J.F.M.; Vlugt, T.J.H.; Gascon, J.; Kapteijin, F. Adsorption-driven heat pumps: the potential of metal-organic frameworks. *Chem Rev* **2015**, 115, 1220–12250. https://doi.org/10.1021/acs.chemrev.5b00059
24. Burtch, N.C.; Jasuja, H.; Walton, K.S. Water stability and adsorption in metal-organic frameworks. *Chem Rev* **2014**, 114, 10575–10612. https://doi.org/10.1021/cr5002589
25. Alayli, Y.; Hadji, N.E.; Leblond, J. A new process for the extraction of water from air. *Desalination* **1987**, 67, 227–229. https://doi.org/10.1016/0011-9164(87)90246-3
26. Kallenberger, P.A.; Fröba, M. Water harvesting from air with a hygroscopic salt in a hydrogel-derived matrix. *Commun Chem* **2018**, 1, 28. https://doi.org/10.1038/s42004-018-0028-9
27. Fathieh, F.; Kalmutzki, M.J.; Kapustin, E.A.; Waller, P.J.; Yang, J.; Yaghi, O.M. Practical water production from desert air. *Sci Adv* **2018**, 4, No. eaat3198. https://doi.org/10.1126/sciadv.aat3198
28. Zhou, X.Y.; Lu, H.Y.; Zhao, F.; Yu, G.H. Atmospheric water harvesting: a review of material and structural designs. *ACS materials Lett* **2020**, 2, 671–684. https://doi.org/10.1021/acsmaterialslett.0c00130
29. Rieth, A.J.; Yang, S.; Wang, E.N.; Dincâ, M. Record atmospheric fresh water capture and heat transfer with a material operating at the water uptake reversibility limit. ACS Cent Sci **2017**, 3, 668–672. https://doi.org/10.1021/acscentsci.7b00186
30. Canivet, J.; Bonnefoy, J.; Daniel, C.; Legrand, A.; Coasne, B.; Farrusseng, D. Structure-property relationships of water adsorption in metal-organic frameworks. New J Chem **2014**, 38, 3102–3111. https://doi.org/10.1039/C4NJ00076E
31. Bon, V.; Senkovska, I.; Evans, J.D.; Wöllner, M.; Hölzel, M.; Kaskel, S. Insights into the water adsorption mechanism in the chemically stable zirconium-based MOF DUT-67 – a prospective material for adsorption-driven heat transformations. *J Mater Chem A* **2019**, 7, 12681–12690. https://doi.org/10.1039/C9TA00825J
32. Furukawa, H.; Gandara, F.; Zhang, Y.B.; Jiang, J.; Queen, W.L.; Hudson, M.R.; Yaghi, O.M. Water adsorption in porous metal-organic frameworks and related materials. *J Am Chem Soc* **2014**, 136, 4369–4381. https://doi.org/10.1021/ja500330a
33. Küsgens, P.; Rose, M.; Senkovska, I.; Fröde, H.; Henschel, A.; Siegle, S.; Kaskel, S. Characterization of metal-organic frameworks by water adsorption. *Microporous Mesoporous Mater* **2009**, 120, 325–330. https://doi.org/10.1016/j.micromeso.2008.11.020

34. Düren, T.; Bae, Y.-S.; Snurr, R.Q. Using molecular simulation to characterise metal-organic frameworks for adsorption applications. *Chem Soc Rev* **2009**, 38, 1237–1247. https://doi.org/10.1039/b803498m
35. Canivet, *J.*; Fateeva, A.; Guo, Y.M.; Coasne, B.; Farrusseng, D. Water adsorption in MOFs: fundamentals and applications. *Chem Soc Rev* **2014**, 43, 5594–5617. https://doi.org/10.1039/C4CS00078A
36. Logan, M.W.; Langevin, S.; Xia, Z.Y. Reversible atmospheric water harvesting using metal-organic frameworks. *Sci Rep* **2020**, 10, 1492. https://doi.org/10.1038/s41598-020-58405-9
37. Chen, Z.J.; Wang, X.J.; Islamoglu, T.; Farha, O.K. Green synthesis of a functionalized zirconium-based metal-organic framework for water, and ethanol adsorption. *Inorganics* **2019**, 7, 56. https://doi.org/10.3390/inorganics7050056
38. Zhao, T.; Jeremias, F.; Boldog, I.; Nguyen B.; Henninger, S.K.; Janiak C. High-yield, fluoride-free and large-scale synthesis of MIL-101(Cr). *Dalton Trans* **2015**, 44, 16791–16801. https://doi.org/10.1039/C5DT02625C
39. Ren, J.; Dyosiba, X.; Musyoka, N.M.; Langmi, H.W.; North, B.C.; Mathe, M. Green synthesis of chromium-based metal-organic framework (Cr-MOF) from waste polyethylene terephthalate (PET) bottles for hydrogen storage applications. *Inter J Hydrogen Energy* **2016**, 41, 18141–18146. https://doi.org/10.1016/j.ijhydene.2016.08.040
40. Ren, J.; Dyosiba, X.; Musyoka, N.M.; Langmi, H.W.; Mathe, M.; Liao, S. Review on the current practices and efforts towards pilot-scale production of metal-organic frameworks (MOFs). *Coord Chem Rev* **2017**, 352, 187–219. https://doi.org/10.1016/j.ccr.2017.09.005